

Role of PIM2 in acute lung injury induced by sepsis

JUNCAI DING^{1,2}, XIUFANG YANG², HUIJUAN HUANG² and BO WANG³

¹Department of Pediatrics, The First Affiliated Hospital of Jinan University, Guangzhou, Guangdong 510630; ²Department of Pediatrics, Zhongshan People's Hospital Affiliated to Sun Yat-sen University, Zhongshan, Guangdong 528403; ³Department of Pediatrics, Guangdong Women and Children Hospital, Guangzhou, Guangdong 511442, P.R. China

Received December 1, 2021; Accepted March 28, 2022

DOI: 10.3892/etm.2022.11480

Abstract. Pediatric sepsis can cause lung damage leading to death in children. In addition, its complicated pathogenesis currently presents a difficult problem in the medical field. Proviral integrations of Moloney virus 2 (PIM2) is a prognostic marker of pediatric sepsis; therefore, the aim of the present study was to investigate the role of PIM2 in lung injury caused by pediatric sepsis. To meet this aim, the expression of PIM2 in lipopolysaccharide (LPS)-induced BEAS-2B pulmonary epithelial cells was detected using reverse transcription-quantitative (RT-q)PCR and western blotting. Subsequently, the expression of PIM2 was inhibited using the cell transfection technique. Cell Counting Kit-8, TUNEL and western blotting, use of a fluorescence kit, ELISA detection kits were used to detect the expression of inflammatory- and cell injury-associated indicators following PIM2 inhibition. In addition, the expression of proteins known to be associated with the Toll-like receptor 2 (TLR2)/myeloid differentiation primary response 88 (MyD88) pathway were also assessed using western blotting. Finally, the simultaneous inhibition of PIM2 expression and overexpression of TLR2 were investigated in an attempt to elucidate the underlying mechanism. The expression level of PIM2 was revealed to be increased in LPS-induced BEAS-2B cells. Interference with PIM2 expression led to an increase in BEAS-2B cell viability, the inhibition of apoptosis and a reduction in oxidative stress and the inflammatory response. These processes were also revealed to be accomplished via downregulation of the TLR2/MyD88 signaling pathway. Overall, the present study demonstrated that knockdown of PIM2 alleviated LPS-induced bronchial epithelial cell injury by inhibiting the TLR2/MyD88 pathway.

Introduction

Sepsis is a systemic inflammatory syndrome caused by infection that provides a major cause of mortality in children (1). A previous study has indicated that there are ~48.9 million patients with sepsis worldwide, including ~11 million sepsis deaths, which account for 19.7% of the total global death (2). Patients with severe sepsis can experience a complicated pathogenesis that also comprises functional impairment of multiple organs (3). The lung is the main organ of sepsis, and the most common complication of sepsis is acute lung injury (ALI) (4). The clinical manifestations of ALI are progressive hypoxemia and respiratory distress, which may lead to acute respiratory distress syndrome (ARDS) if the disease progresses (5). Due to the complex pathogenesis of pediatric sepsis, which causes great damage to the body tissues and organs and is difficult to treat, sepsis remains a difficult problem that needs to be resolved in the medical field in the world at present (6).

Proviral integrations of Moloney virus 2 (PIM2) is a serine/threonine protein kinase that exists on the X chromosome in three isotypes (34 kDa, 37 kDa and 40 kDa) and is highly expressed in lymphatic and brain tissues (7). PIM2 fulfills important roles in cell proliferation, apoptosis and other biological processes including migration, invasion and autophagy (8). At present, the majority of studies on PIM2 focus on its role in hematological malignancies and solid tumors, and it has been revealed that PIM2 exerts a promoting effect on the occurrence and development of multiple myeloma (9), prostate cancer (10), liver cancer (11) and other tumors, including lung cancer, ovarian cancer. However, previously published studies have indicated that PIM2 may exert certain immune regulation effects (12,13). Yang *et al* (14) demonstrated that PIM2 can induce interleukin (IL)-6 production through the IL-1 β or TNF- α pathway, thereby regulating the occurrence of inflammatory diseases. A previous study revealed that PIM2 is a prognostic marker of pediatric sepsis (15). Inhibition of PIM2 has also been indicated to alleviate asthma symptoms and to improve airway hyper-responsiveness and airway inflammation (16). Collectively, these data have indicated that PIM2 may exhibit a role in pediatric sepsis.

Moreover, low doses of PIM2 protein have been demonstrated to have a protective effect on oxidative stress-induced neuronal cell death (17), and PIM2 expression is significantly upregulated in lipopolysaccharide (LPS)-induced mouse macrophages (18). Knockdown of PIM2 causes a marked

Correspondence to: Dr Bo Wang, Department of Pediatrics, Guangdong Women and Children Hospital, 521 Xingnan Road, Panyu, Guangzhou, Guangdong 511442, P.R. China
E-mail: wangbo1599@163.com

Key words: pediatric sepsis, proviral integrations of Moloney virus 2, cell injury, Toll-like receptor 2/myeloid differentiation primary response 88 pathway

reduction in the expression of IL-1 β and NLR family pyrin domain-containing 3 (NLRP3) inflammasome in LPS-induced macrophages, thereby alleviating LPS-induced ARDS (18). In addition, PIM2 expression has been revealed to be elevated in lung cancer tissue, which may have a specific regulatory role in the occurrence and development of lung cancer (19). Therefore, it is reasonable to hypothesize that PIM2 is involved in LPS-induced injury of pulmonary epithelial cells.

The present study explored the role of PIM2 in LPS-induced *in vitro* ALI cell model in bronchial epithelial cells and its underlying mechanisms so as to provide a theoretical basis for the treatment of lung injury caused by pediatric sepsis.

Materials and methods

Cell culture. Human BEAS-2B pulmonary epithelial cells, obtained from American Type Culture Collection, were cultured in Gibco[®] DMEM with 10% FBS (both Thermo Fisher Scientific, Inc.) in a humidified incubator at 37°C and an atmosphere of 5% CO₂. BEAS-2B cells were induced by LPS (at concentrations of 0, 2.5, 5 and 10 μ g/ml) at 37°C for 12 h to create an *in vitro* ALI model.

Reverse transcription-quantitative (RT-q)PCR. Total RNA from the cells was isolated using Invitrogen[®] TRIzol[®] reagent (Thermo Fisher Scientific, Inc.). cDNA was synthesized using a Fermentas[®] First-Strand cDNA Synthesis kit (Thermo Fisher Scientific, Inc.). A SYBR Green Master Mix (20 μ l; Invitrogen; Thermo Fisher Scientific, Inc.) was used to perform the PCR. The reaction thermocycling conditions were as follows: 95°C for 5 min, followed by 40 cycles of 94°C for 15 sec, 60°C for 20 sec and 72°C for 40 sec. RT-qPCR using an Applied Biosciences[®] ABI StepOnePlus Real-time PCR system (Thermo Fisher Scientific, Inc.) was used to detect the transcripts. The expression level was calculated using the 2^{- $\Delta\Delta$ Cq} method (20), and the levels were normalized against GAPDH as the housekeeping gene. The results are expressed as the fold-changes. The sequences were designed by Guangzhou RiboBio Co., Ltd. PIM2 forward, 5'-CGTGGAGTTGTCCATCGTG-3', and reverse, 5'-AAGGGAATGTCCCCACACAC-3'; Toll-like receptor 2 (TLR2) forward, 5'-TTGTGACCGCAA TGGTATCT-3', and reverse, 5'-TGTTGGACAGGTCAAGGC T-3'; GAPDH forward, 5'-CATGAGAAGTATGACAACAGC CT-3', and reverse, 5'-AGTCCTTCCACGATACCAAAGT-3'.

Western blotting. Cells were washed with PBS and collected in RIPA lysis buffer (Cell Signaling Technology, Inc.). Subsequently, the cells were centrifuged at 16,000 x g for 10 min at 4°C, and the supernatant was collected for western blotting. A bicinchoninic acid protein assay kit (Thermo Fisher Scientific, Inc.) was used to detect the protein concentrations. Protein (20 μ g per lane) samples were analyzed by (either 10 or 12%) SDS-polyacrylamide gel electrophoresis and subsequently transferred onto a PVDF membrane. The membranes were then blocked in 5% skimmed milk powder for 1 h at room temperature and subsequently incubated overnight at 4°C with primary antibodies, including anti-PIM2 (cat. no. ab129057), anti-Bcl-2 (cat. no. ab32124), anti-Bax (cat. no. ab182733), anti-cleaved caspase-3 (cat. no. ab32042),

anti-caspase-3 (cat. no. ab32351), anti-cleaved caspase-9 (cat. no. ab2324), anti-caspase-9 (cat. no. ab32539), anti-mono-cycte chemoattractant protein-1 (MCP-1; cat. no. ab214819), anti-inducible nitric oxide synthase (iNOS; cat. no. ab178945), anti-cyclooxygenase (COX)-2 (cat. no. ab179800), anti-TLR2 (cat. no. ab68159), anti-myeloid differentiation primary response 88 (MyD88; cat. no. ab133739), anti-phosphorylated (p)-p65 (cat. no. ab76302), anti-p65 (cat. no. ab32536) and anti-GAPDH (cat. no. ab9485) all from Abcam (all dilution, 1:1,000). Membranes were subsequently incubated with horse-radish peroxidase-conjugated secondary antibody (1:5,000 dilution; cat. no. ab150077, Abcam) at room temperature for 1 h. The protein bands were colored using an enhanced chemiluminescence kit (Bio-Rad Laboratories, Inc.) and ImageJ 1.50i (National Institutes of Health) gel analysis software was used to analyze the bands. GAPDH was used as the loading control.

Cell transfection. Cells were transfected either with PIM2-small interfering (si)RNAs or with scrambled negative control (NC) siRNA (200 nM; Shanghai GenePharma Co., Ltd.). Transfection of pcDNA3.1 overexpression vector (GenScript) encoding the full-length TLR2 for overexpression of TLR2 or the empty plasmid negative control (NC) produced by Shanghai GenePharma Co., Ltd all at the concentration of 20 nM was performed using the transfection reagent Lipofectamine[™] 2000 (Invitrogen; Thermo Fisher Scientific, Inc.) at 37°C for 24 h. The sequences of the si-PIM2-1 and si-PIM2-2 primers were as follows: Si-PIM2-1, 5'-ACCUUC UCCCCGACCCUCAdTdT-3' (sense), and 5'-UGAGGGUCG GGAAGAAGGUdTdT-3' (antisense); si-PIM2-2, 5'-CUUGGU UUUACAGGUCAUUdTdT-3' (sense), and 5'-AAUGACCUG UAAAACCAAGdCdT-3' (antisense); si-NC, 5'-UUCUCC GAACGUGUCACGUTT-3' (sense), and 5'-ACGUGACAC GUUCGGAGAATT-3' (antisense). At 48 h after transfection, subsequent experiments were conducted.

Cell Counting Kit-8 (CCK-8) assay. Cells were seeded and cultured at a density of 5x10³/well in 96-well microplates (Corning, Inc.). Subsequently, the cells were treated with LPS for 12 h, and transfected accordingly as described above. CCK-8 reagent (10 μ l; Beyotime Institute of Biotechnology) was added to each well, and the cells were subsequently cultured for 2 h. A microplate reader (Bio-Rad Laboratories, Inc.) was used to analyze the absorbance at 450 nm.

TUNEL staining. Apoptosis was assessed using a TUNEL assay kit (Beyotime Institute of Biotechnology) in accordance with the manufacturer's protocol. Cells were washed with PBS and then fixed with 4% paraformaldehyde for 30 min at room temperature. Subsequently, cells were incubated with permeabilization solution for 5 min at room temperature followed by TUNEL solution for 1 h at 37°C. Subsequently, 50 μ l DAB substrate was added for 10 min at 15°C, and hematoxylin was used to re-stain the cells for 10 sec at room temperature. Slides were mounted using glycerol. The cells were observed under glass coverslip with PBS under an inverted microscope (magnification, x200; Olympus Corporation). A total of three fields were randomly selected for analysis of the images.

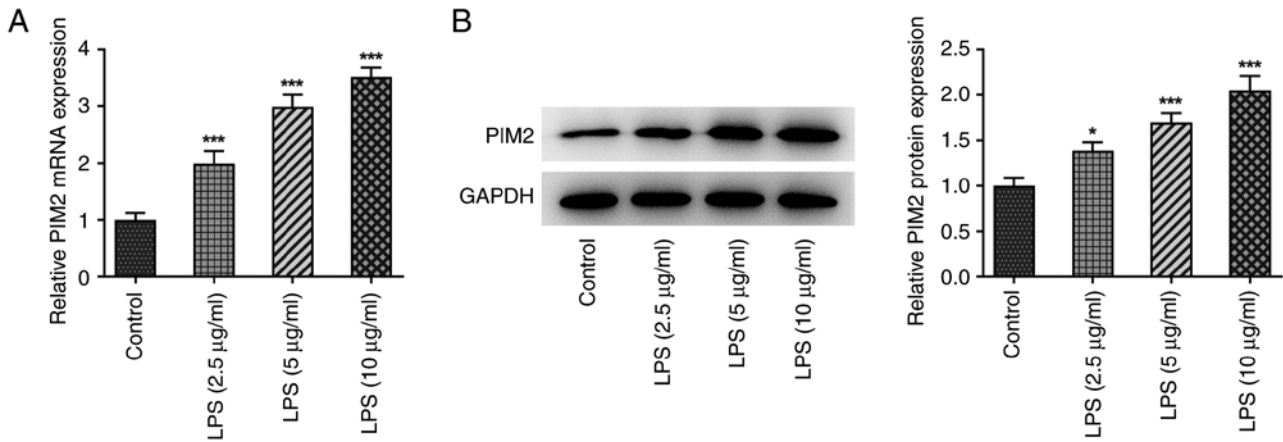


Figure 1. Expression of PIM2 in LPS-induced BEAS-2B cells. (A) Reverse transcription-quantitative PCR and (B) western blotting detected the expression levels of PIM2 mRNA and protein, respectively, in LPS-induced BEAS-2B cells. * $P < 0.05$ and *** $P < 0.001$ vs. control. PIM2, Proviral integrations of Moloney virus 2; LPS, lipopolysaccharide.

Detection of reactive oxygen species (ROS) production.

Intracellular ROS levels were analyzed using the fluorescence intensity of 2,7-dichlorofluorescein. BEAS-2B cells cultured on 6-well chamber slides (1×10^6) were washed with PBS three times for 5 min/wash, and the slides were incubated with the fluorescent probe 2,7-dichlorodihydrofluorescein diacetate (1:1,000 dilution) at 37°C for 30 min in the dark. The fluorescence signals were analyzed on a BD FACSCanto™ Clinical Flow Cytometry System (BD Biosciences), and FlowJo version 7.6 software (FlowJo LLC) was used to analyze the data.

Detection of superoxide dismutase (SOD) and plasma glutathione peroxidase (GSH-Px) production.

BEAS-2B cells were centrifuged at $1,600 \times g$ for 10 min at 4°C and the cellular supernatant was collected in order to detect the levels of SOD (cat. no. HM10163) and GSH-Px (cat. no. HM10129) using ELISA kits (Bio-Swamp; Wuhan Bientle Biotechnology Co., Ltd.) according to the manufacturer's instructions. A microplate reader was subsequently used to measure the absorbance at 450 nm absorbance wavelength.

ELISA. Briefly, BEAS-2B cells were seeded into 96-well plates (5×10^3 cells/well). Following treatment, cell supernatant was collected after centrifugation at $2,000 \times g$ for 5 min at 4°C . The intracellular concentrations of IL-1 β (cat. no. 557953), IL-6 (cat. no. 555220) and TNF- α (cat. no. 555212) were assessed using BD OptEIA™ Human IL-1 β ELISA Set II, BD OptEIA™ Human IL-6 ELISA Set and BD OptEIA™ Human TNF ELISA Set (BD Biosciences), and all procedures were performed according to the manufacturer's instructions.

Statistical analyses. Statistical analyses were performed using SPSS software (version 18.0; SPSS, Inc.). The data are presented as the mean \pm SD from at least three independent experiments. Comparisons between two groups were performed using unpaired Student's t-test, whereas comparisons among multiple groups were performed using one-way ANOVA followed by a Tukey's post hoc test. $P < 0.05$ was considered to indicate a statistically significant difference.

Results

Interference with PIM2 increases the viability of LPS-induced BEAS-2B cells. First, expression of PIM2 was detected using both RT-qPCR and western blotting in BEAS-2B cells induced by different concentrations of LPS (0, 2.5, 5 and 10 $\mu\text{g/ml}$). The results obtained demonstrated that, compared with the control group, the expression level of PIM2 increased markedly in concert with the increases in concentration of LPS, which was used to induce the cells (Fig. 1A and B). Since PIM2 expression was the most significantly increased when induced using 10 $\mu\text{g/ml}$ LPS, LPS at this concentration was consequently selected for subsequent experiments. PIM2 expression was then inhibited using the cell transfection technique. RT-qPCR and western blotting were used to determine the efficiency of siRNA interference of the cells. The results demonstrated that the expression level of PIM2 in the si-PIM2-1 and si-PIM2-2 groups were significantly decreased compared with the si-NC group, indicating that the interference was successful. In addition, as the expression of PIM2 in the si-PIM2-1 group was decreased more obviously compared with the si-PIM2-2 group, si-PIM2-1 was selected to be used in the follow-up experiments (Fig. 2A and B).

The CCK-8 assay results demonstrated that cell viability was significantly decreased after LPS induction compared with the control group. Compared with the LPS + si-NC treatment group, the cell viability of the LPS + si-PIM2 group was significantly increased (Fig. 2C). Subsequently, the TUNEL assay results indicated that, compared with the control group, apoptosis was significantly increased in the BEAS-2B cells induced with LPS only (Fig. 2D and E). In addition, western blotting demonstrated that LPS-induced cells demonstrated a significant decrease in Bcl-2 expression and significant increases in Bax and cleaved caspase-3 and -9 expression levels compared with the control group (Fig. 2F and G). Moreover, compared with the LPS + si-NC group, PIM2 interference significantly reduced the level of apoptosis LPS + si-PIM2 group, which was accompanied by a significantly increased level of Bcl-2 expression and decreased expression levels of Bax and cleaved caspase-3

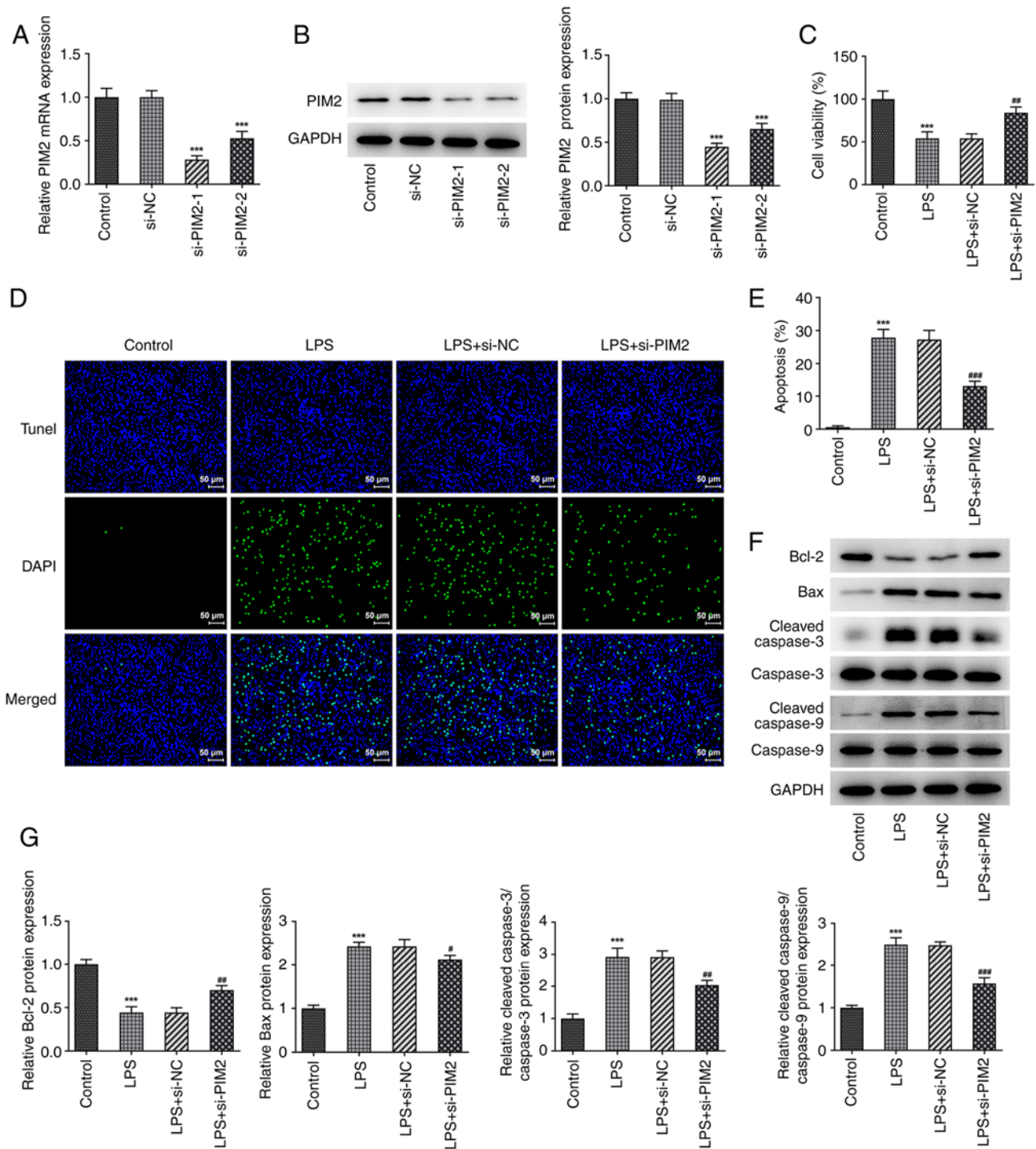


Figure 2. Interference with PIM2 increases viability of LPS-induced BEAS-2B cells. (A) Reverse transcription-quantitative PCR and (B) western blotting detected the expression levels of PIM2 mRNA and protein, respectively, after transfection of PIM2. $^{***}P < 0.001$ vs. si-NC. (C) Cell Counting Kit-8 detected the viability in LPS-induced BEAS-2B cells after transfection of PIM2. (D and E) TUNEL assay detected the apoptosis of LPS-induced BEAS-2B cells after transfection of PIM2 (scale bar, 50 μ m). (F) Western blotting detected the expression levels of apoptosis-related proteins (Bcl-2, Bax and cleaved caspase-3/caspase-3) in LPS-induced BEAS-2B cells after transfection of PIM2. (G) Statistical analyses of a apoptosis-related protein bands. $^{***}P < 0.001$ vs. control; $^{\#}P < 0.05$, $^{##}P < 0.01$, $^{###}P < 0.001$ vs. LPS + si-NC. PIM2, Proviral integrations of Moloney virus 2; LPS, lipopolysaccharide; NC, negative control; si-, small interfering.

and -9 (Fig. 2D-G). PIM2 silencing exacerbated the viability of LPS-treated BEAS-2B cells.

Interference with PIM2 inhibits oxidative stress and the inflammatory response of LPS-induced BEAS-2B cells. ROS expression levels were detected using a fluorescence kit, and

the expression levels of SOD and GSH-Px were detected using corresponding kits. The results obtained demonstrated that, ROS expression in the LPS-induced BEAS-2B cells significantly increased following LPS induction compared with the control group; whereas the expression levels of SOD and GSH-Px were significantly decreased. Compared

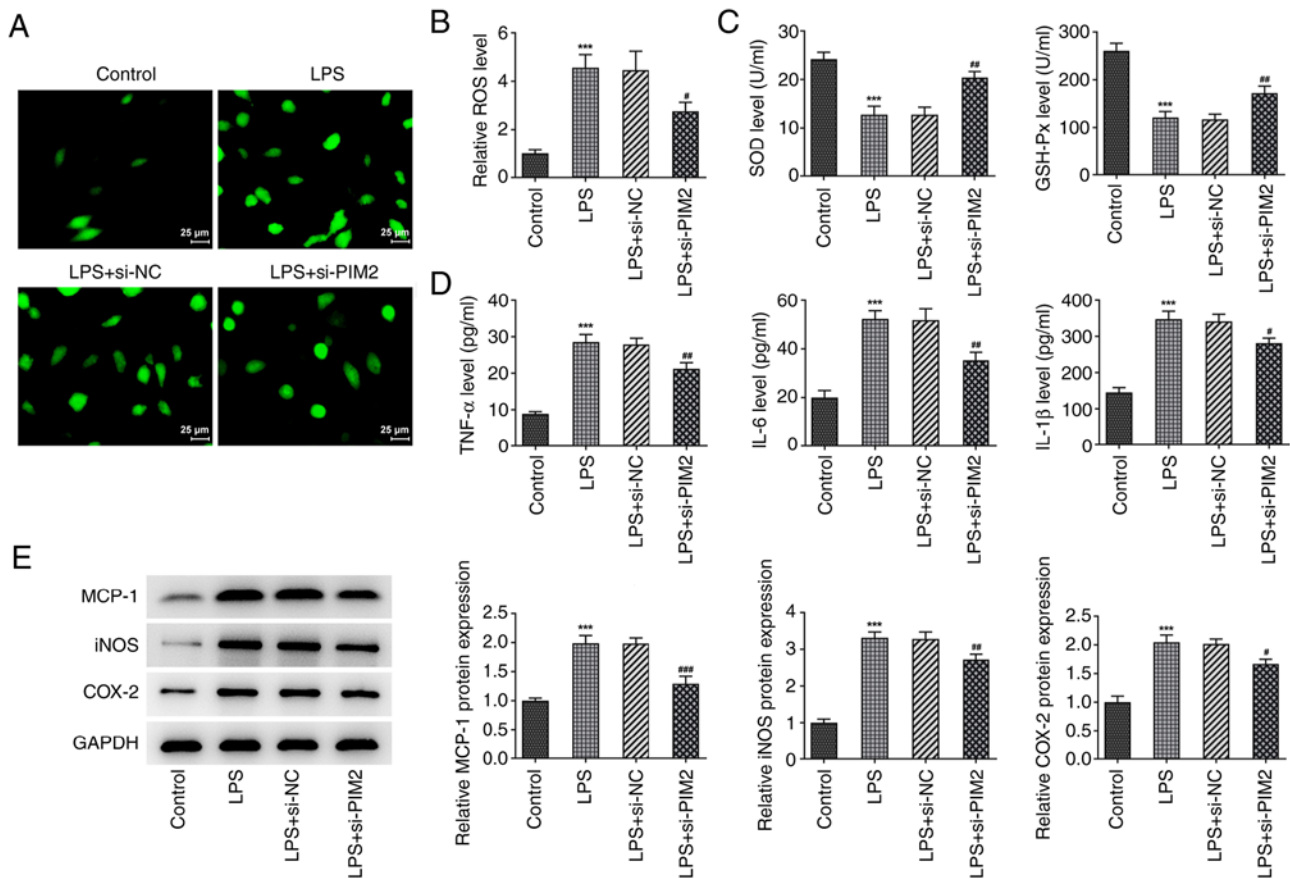


Figure 3. Interference with PIM2 inhibits oxidative stress and inflammatory response of LPS-induced BEAS-2B cells. (A) A DCFH-DA kit was used to detect the expression of ROS and (B) was quantified. (C) SOD and GSH-Px kits were used to detect the expression of SOD and GSH-Px. (D) ELISA was used to detect the expression of inflammation factors, TNF- α , IL-6 and IL-1 β . (E) Western blotting detected the expression of inflammation-related proteins (MCP-1, iNOS and COX-2) in LPS-induced BEAS-2B cells after transfection. *** $P < 0.001$ vs. control; # $P < 0.05$, ## $P < 0.01$, ### $P < 0.001$ vs. LPS + si-NC. PIM2, Proviral integrations of Moloney virus 2; LPS, lipopolysaccharide; NC, negative control; si-, small interfering; ROS, reactive oxygen species; SOD, superoxide dismutase; GSH-Px, glutathione peroxidase; IL, interleukin; MCP-1, monocyte chemoattractant protein-1; iNOS, inducible nitric oxide synthase; COX-2, cyclooxygenase.

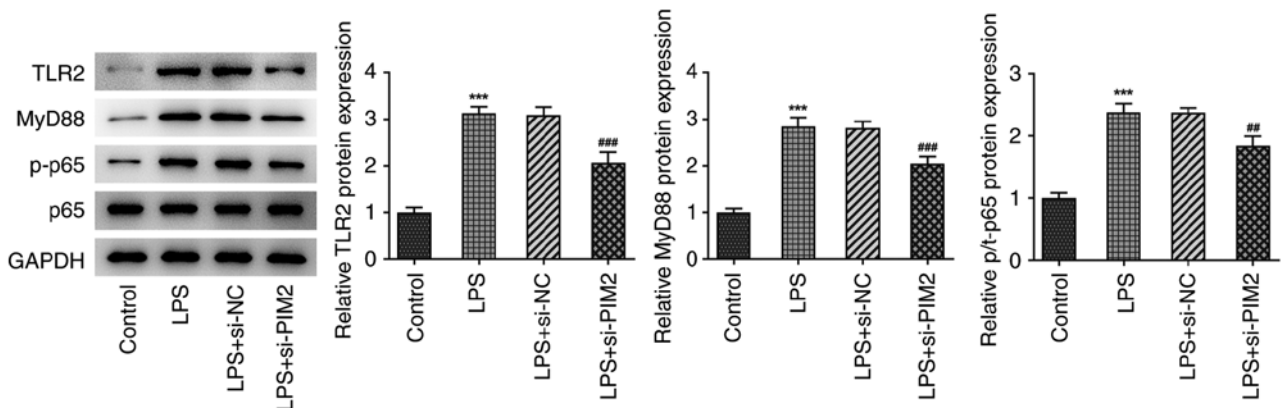


Figure 4. Interference with PIM2 inhibited the activation of the TLR2/MyD88 signaling pathway in LPS-induced BEAS-2B cells. Western blotting detected the expression of TLR2/MyD88 signaling pathway associated proteins, TLR2, MyD88 and p/t-P65. *** $P < 0.001$ vs. control; ## $P < 0.01$, ### $P < 0.001$ vs. LPS + si-NC. p-, phosphorylated; t-, total; PIM2, Proviral integrations of Moloney virus 2; LPS, lipopolysaccharide; NC, negative control; si-, small interfering; TLR2, Toll-like receptor 2; MyD88, myeloid differentiation primary response 88.

with the LPS + si-NC group, the ROS expression levels in the LPS + si-PIM2 group were significantly decreased after interfering with PIM2 expression, whereas those of SOD and GSH-Px were significantly increased (Fig. 3A-C). In addition, the expression levels of TNF- α , IL-6 and IL-1 β were

significantly increased following LPS induction compared with the control group. However, following PIM2 interference, the expression levels of these factors were significantly decreased in the LPS + si-PIM2 group compared with the LPS + si-NC group (Fig. 3D). Finally, the expression levels

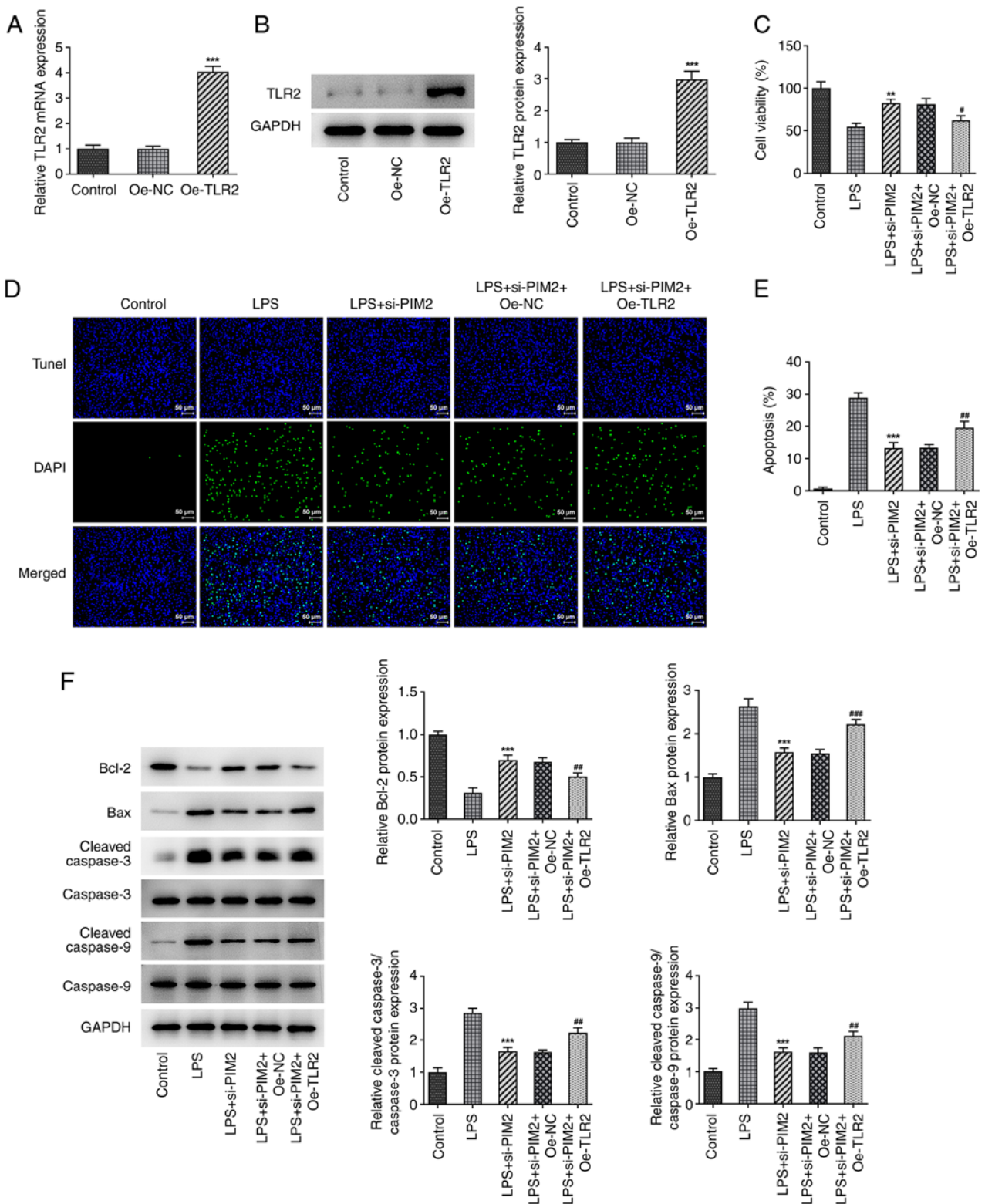


Figure 5. Upregulation of TLR2 reverses the inhibitory effect of PIM2 interference on BEAS-2B cell viability. (A) Reverse transcription-quantitative PCR and (B) western blotting detected the expression of TLR2 mRNA and protein, respectively, after transfection of TLR2. *** $P < 0.001$ vs. si-NC. (C) Cell Counting Kit-8 detected the viability in LPS-induced BEAS-2B cells after transfection. (D and E) TUNEL assay detected the apoptosis of LPS-induced BEAS-2B cells after transfection (scale bar, 50 μm). (F) Western blotting detected the expression levels of apoptosis-related proteins in LPS-induced BEAS-2B cells after transfection. ** $P < 0.01$, *** $P < 0.001$ vs. LPS; # $P < 0.05$, ## $P < 0.01$, ### $P < 0.001$ vs. LPS + si-PIM2 + Oe-TLR2. PIM2, Proviral integrations of Moloney virus 2; LPS, lipopolysaccharide; NC, negative control; si-, small interfering; TLR2, Toll-like receptor 2; oe, overexpression.

of the inflammation-associated proteins MCP-1, iNOS and COX-2 were revealed to be consistent with the trends of TNF- α , IL-6 and IL-1 β as determined from western

blotting (Fig. 3E). In conclusion, PIM2 knockdown ameliorated LPS-evoked oxidative stress and inflammatory response in BEAS-2B cells.

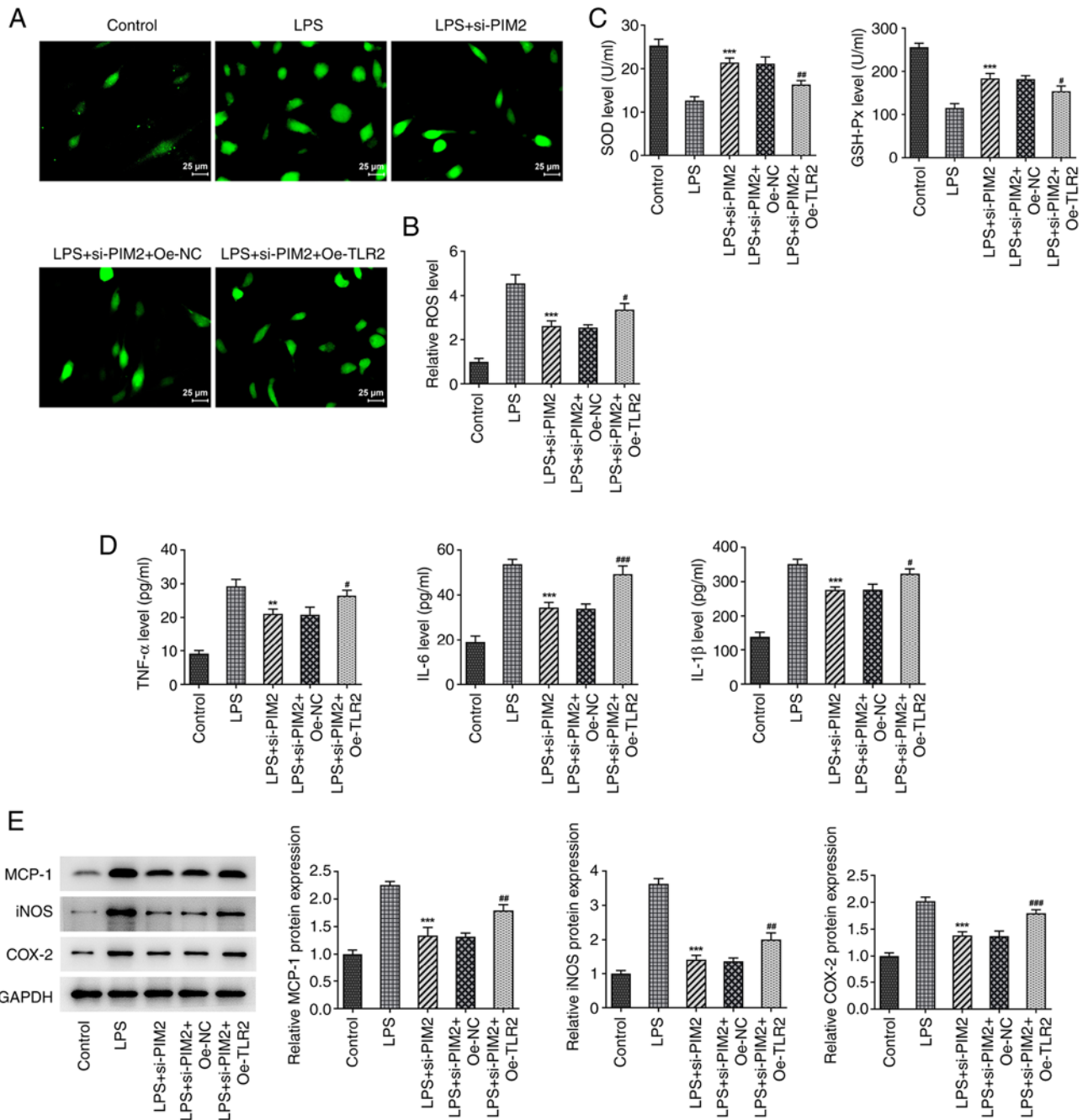


Figure 6. Upregulation of TLR2 reverses the inhibitory effect of PIM2 interference on BEAS-2B cell oxidative stress and inflammation. (A) DCFH-DA kit was used to detect and (B) quantify the expression levels of ROS (scale bar, 25 μ m). (C) SOD and GSH-Px kits were used to detect the expression levels of SOD and GSH-Px. (D) ELISA was used to detect the expression of inflammation factors TNF- α , IL-6 and IL-1 β . (E) Western blotting detected the expression of inflammation-related proteins (MCP-1, iNOS and COX-2) in LPS-induced BEAS-2B cells after transfection. **P<0.01, ***P<0.001 vs. LPS; #P<0.05, ##P<0.01, ###P<0.001 vs. LPS + si-PIM2 + Oe-TLR2. PIM2, Proviral integrations of Moloney virus 2; LPS, lipopolysaccharide; NC, negative control; si-, small interfering; ROS, reactive oxygen species; SOD, superoxide dismutase; GSH-Px, glutathione peroxidase; IL, interleukin; MCP-1, monocyte chemoattractant protein-1; iNOS, inducible nitric oxide synthase; COX-2, cyclooxygenase; Oe, overexpression.

Interference with PIM2 inhibits activation of the TLR2/MyD88 signaling pathway in LPS-induced BEAS-2B cells. The western blotting results demonstrated that the expression levels of TLR2, MyD88 and p-P65 in BEAS-2B cells were significantly increased following LPS induction compared with the control, indicating that LPS could induce activation of the TLR2/MyD88 pathway. Compared with the LPS + si-NC treatment group, the expression levels of TLR2, MyD88 and p-P65 were significantly inhibited following PIM2

expression (Fig. 4). These results preliminarily suggested that PIM2 interference was able to inhibit the activation of TLR2/MyD88 pathway. Taken together, PIM2 depletion inactivated TLR2/MyD88 signaling in LPS-treated BEAS-2B cells.

Upregulation of TLR2 reverses the inhibitory effect of PIM2 interference on BEAS-2B cell damage. Subsequently, the cells were grouped into control, LPS, LPS + si-PIM2,

LPS + si-PIM2 + overexpression (Oe)-NC and LPS + si-PIM2 + Oe-TLR2 treatment groups to further explore the mechanism of PIM2 in LPS-induced BEAS-2B cell injury. First, TLR2 was overexpressed using the cell transfection technique, and the transfection efficiency was confirmed using RT-qPCR and western blotting assays (Fig. 5A and B). It was revealed that, compared with the LPS + si-PIM2 + Oe-NC treatment group, the LPS + si-PIM2 + Oe-TLR2 group had a significantly decreased cell viability (Fig. 5C) and significantly increased levels of apoptosis (Fig. 5D and E); this was accompanied by a significant decrease of Bcl-2 expression, and significantly increased levels of Bax and cleaved/total caspase-3 and -9 expression (Fig. 5F). Subsequently, the levels of the oxidative stress-associated indicators ROS, SOD and GSH-Px (Fig. 6A-C), as well as the inflammatory indicators TNF- α , IL-6 and IL-1 β , were examined (Fig. 6D). The results demonstrated that the expression levels of ROS were significantly increased in the LPS + si-PIM2 + Oe-TLR2 group compared with the LPS + si-PIM2 + Oe-NC group (Fig. 6A and B), while the expression levels of SOD and GSH-Px were significantly decreased (Fig. 6C). In addition, the expression levels of TNF- α , IL-6 and IL-1 β were significantly increased in the LPS + si-PIM2 + Oe-TLR2 group compared with the LPS + si-PIM2 + Oe-NC group (Fig. 6D). The expression trends of MCP-1, iNOS and COX-2 were revealed to be consistent with those of the inflammatory factors TNF- α , IL-6 and IL-1 (Fig. 6E). Collectively, these results suggested that upregulation of TLR2 could reverse the inhibitory effect of PIM2 interference on cell damage. Overall, TLR2 elevation offset the mitigated BEAS-2B cell injury due to PIM2 deficiency.

Discussion

A large number of inflammatory factors produced by sepsis are able to enter the lung tissue via the blood circulation, and accumulate in lung tissue to produce pulmonary inflammatory reactions, thereby damaging the pulmonary capillary endothelial cells and pulmonary epithelial cells, ultimately causing sepsis combined with ALI (21,22). Children's bodily functions are not fully developed, and for them, sepsis is more dangerous; therefore, pediatric sepsis may lead to more serious organ damage, such as ALI, which is more difficult to treat (23). Consequently, it is important to explore the underlying mechanism through which sepsis causes lung injury in children.

In the set of experiments performed in the present study, LPS-induced BEAS-2B cells were used to simulate a model of ALI induced by sepsis (24). In a study by Wang *et al* (24), LPS at 10 $\mu\text{g/ml}$ was selected for induction, and LPS at this concentration could induce the model of extracorporeal pneumonia. In addition, the present study selected 2.5, 5 and 10 $\mu\text{g/ml}$ LPS for induction, and demonstrated that PIM2 expression was most significantly increased after 10 $\mu\text{g/ml}$ LPS induction. Therefore, 10 $\mu\text{g/ml}$ LPS was selected in the present study. The results obtained revealed that after LPS induction, cell viability decreased significantly, the levels of apoptosis increased and oxidative stress and inflammation occurred in the cells. Taken together, these results demonstrated that the present model had been successfully induced.

PIM2 is a prognostic marker of pediatric sepsis (15); although, to the best of our knowledge, the role of PIM2 both in pediatric sepsis and in lung injury caused by sepsis has yet to be reported. PIM2 has been reported to be highly expressed in lung cancer, and microarray analysis has indicated that it is associated with cell proliferation (25). In addition, PIM1 and PIM2 share a high degree of amino acid sequence homology, and their functions are fundamentally the same (26). PIM1 has been demonstrated to inhibit the inflammatory response and cell viability of BEAS-2B cells in obstructive pulmonary disease, thereby inducing cell death (27). Therefore, it was possible to hypothesize that PIM2 also fulfills a role in LPS-induced BEAS-2B cells. In the present study, PIM2 expression was significantly increased after the BEAS-2B cells had been induced by LPS. Following the inhibition of PIM2 expression, cell viability was increased, apoptosis was decreased and the cellular inflammatory response was also decreased. Moreover, a previously published study has indicated that PIM2 interference can inhibit the expression of IL-1 β and NLRP3 in LPS-induced macrophages, thereby inhibiting inflammatory responses (18). Similarly, the present set of experiments revealed that the expression levels of TNF- α , IL-6 and IL-1 β in LPS-induced BEAS-2B cells were decreased after interfering with PIM2 expression, and the inflammatory response and oxidative stress response were both inhibited. Collectively, these results demonstrated that PIM2 interference could inhibit LPS-induced cell damage.

Subsequently, the present study sought to unravel the underlying regulatory mechanism of PIM2. It was revealed that the TLR2/MyD88 signaling pathway was abnormally expressed during the entire process. The TLR2/MyD88 inflammatory pathway forms an important part of the body's inflammatory response (28). TLR2 interacts with MyD88, forming a complex that activates downstream signal transduction through a series of phosphorylation processes, which ultimately activates the expression of various genes, including those of TNF- α , IL-1, IL-6 and adhesion molecules, thereby inducing corresponding inflammatory responses (29). It has also been demonstrated that inhibition of the TLR2/MyD88 pathway alleviates LPS-induced ALI in a rat model (30). It is also hypothesized that TLR2 may bind LPS through the LPS-binding protein (31). In the present set of experiments, the TLR2/MyD88 signaling pathway was revealed to be activated following LPS-induced injury of the BEAS-2B cells.

PIM2 has been indicated to regulate the expression of downstream signaling pathways in a TLR2-dependent manner (32). In addition, a previously published study demonstrated that PIM2 is able to activate the NF- κ B signaling pathway to promote the occurrence of liver cancer (33), and that this activation is caused by the activation of the TLR2/MyD88 signaling cascade (34). Growth differentiation factor 11, a regulator of skin biology, exerts a protective role in LPS-induced lung injury through inhibiting the TLR2/high mobility group box 1/NF- κ B signaling axis (35). Therefore, it was possible to hypothesize that PIM2 may exert a role in ALI caused by pediatric sepsis by effecting downstream regulation of the TLR2/MyD88 signaling pathway. To further confirm this hypothesis, TLR2 was overexpressed, which resulted in a reversal of the inhibition mediated by PIM2 on the LPS-induced inflammatory response, oxidative stress and

apoptosis in BEAS-2B cells. These results revealed that knockdown of PIM2 was able to alleviate LPS-induced pulmonary epithelial cell injury via inhibiting the TLR2/MyD88 pathway.

The present study has certain limitations. The conclusions of the current study were not verified in animal experiments, so these will be verified in the following experiments. In addition, the BEAS-2B cell line was used in our experiment, which should be verified in more cell lines. Our research group will also discuss other cell lines in the future.

In conclusion, the present study confirmed that knockdown of PIM2 was able to alleviate LPS-induced pulmonary epithelial cell injury via inhibiting the TLR2/MyD88 pathway. The present study has therefore provided a potential novel basis for the treatment of ALI caused by pediatric sepsis.

Acknowledgements

Not applicable.

Funding

No funding was received.

Availability of data and materials

The datasets used and/or analyzed during the current study are available from the corresponding author on reasonable request.

Authors' contributions

JD and XY conceived and designed the study. HH and BW performed the experiments. XY and HH analyzed the experimental data. JD and BW wrote and revised the manuscript. XY and HH confirm the authenticity of all the raw data. All authors have read and approved the final manuscript.

Ethics approval and consent to participate

Not applicable.

Patient consent for publication

Not applicable.

Competing interests

The authors declare that they have no competing interests.

References

- Cecconi M, Evans L, Levy M and Rhodes A: Sepsis and septic shock. *Lancet* 392: 75-87, 2018.
- Rudd KE, Johnson SC, Agesa KM, Shackelford KA, Tsoi D, Kievlan DR, Colombara DV, Ikuta KS, Kisssoon N, Finfer S, *et al*: Global, regional, and national sepsis incidence and mortality, 1990-2017: Analysis for the Global Burden of Disease Study. *Lancet* 395: 200-211, 2020.
- Lelubre C and Vincent JL: Mechanisms and treatment of organ failure in sepsis. *Nat Rev Nephrol* 14: 417-427, 2018.
- Yan XX, Zheng AD, Zhang ZE, Pan GC and Zhou W: Protective effect of pantoprazole against sepsis-induced acute lung and kidney injury in rats. *Am J Transl Res* 11: 5197-5211, 2019.
- Li X, Jamal M, Guo P, Jin Z, Zheng F, Song X, Zhan J and Wu H: Irisin alleviates pulmonary epithelial barrier dysfunction in sepsis-induced acute lung injury via activation of AMPK/SIRT1 pathways. *Biomed Pharmacother* 118: 109363, 2019.
- Uhle F, Lichtenstern C, Brenner T and Weigand MA: Pathophysiology of sepsis. *Anesthesiol Intensivmed Notfallmed Schmerzther* 50: 114-122, 2015 (In German).
- Brault L, Gasser C, Bracher F, Huber K, Knapp S and Schwaller J: PIM serine/threonine kinases in the pathogenesis and therapy of hematologic malignancies and solid cancers. *Haematologica* 95: 1004-1015, 2010.
- Yang T, Ren C, Lu C, Qiao P, Han X, Wang L, Wang D, Lv S, Sun Y and Yu Z: Phosphorylation of HSF1 by PIM2 Induces PD-L1 expression and promotes tumor growth in breast cancer. *Cancer Res* 79: 5233-5244, 2019.
- Fujii S, Nakamura S, Oda A, Miki H, Tenshin H, Teramachi J, Hiasa M, Bat-Erdene A, Maeda Y, Oura M, *et al*: Unique anti-myeloma activity by thiazolidine-2,4-dione compounds with Pim inhibiting activity. *Br J Haematol* 180: 246-258, 2018.
- Ren K, Gou X, Xiao M, He W and Kang J: Pim-2 cooperates with downstream factor XIAP to inhibit apoptosis and intensify malignant grade in prostate cancer. *Pathol Oncol Res* 25: 341-348, 2019.
- Kronsnabl P, Grunweller A, Hartmann RK, Aigner A and Weirauch U: Inhibition of PIM2 in liver cancer decreases tumor cell proliferation in vitro and in vivo primarily through the modulation of cell cycle progression. *Int J Oncol* 56: 448-459, 2020.
- Yin G, Li Y, Yang M, Cen XM and Xie QB: Pim-2/mTORC1 pathway shapes inflammatory capacity in rheumatoid arthritis synovial cells exposed to lipid peroxidations. *Biomed Res Int* 2015: 240210, 2015.
- Deng G, Nagai Y, Xiao Y, Li Z, Dai S, Ohtani T, Banham A, Li B, Wu SL, Hancock W, *et al*: Pim-2 Kinase influences regulatory T cell function and stability by mediating Foxp3 protein N-terminal phosphorylation. *J Biol Chem* 290: 20211-20220, 2015.
- Yang J, Li X, Hanidu A, Htut TM, Sellati R, Wang L, Jiang H and Li J: Proviral integration site 2 is required for interleukin-6 expression induced by interleukin-1, tumour necrosis factor- α and lipopolysaccharide. *Immunology* 131: 174-182, 2010.
- Tonial CT, Costa CAD, Andrades GRH, Crestani F, Bruno F, Piva JP and Garcia PCR: Performance of prognostic markers in pediatric sepsis. *J Pediatr (Rio J)* 97: 287-294, 2021.
- Du W, Chen T, Ni Y, Hou X, Yu Y, Zhou Q, Wu F, Tang W and Shi G: Role of PIM2 in allergic asthma. *Mol Med Rep* 16: 7504-7512, 2017.
- Woo SJ, Shin MJ, Kim DW, Jo HS, In Yong J, Ryu EJ, Cha HJ, Kim SJ, Yeo HJ, Cho SB, *et al*: Effects of low doses of Tat-PIM2 protein against hippocampal neuronal cell survival. *J Neurol Sci* 358: 226-235, 2015.
- Wang F, Xu L, Dong G, Zhu M, Liu L and Wang B: PIM2 deletion alleviates lipopolysaccharide (LPS)-induced respiratory distress syndrome (ARDS) by suppressing NLRP3 inflammasome. *Biochem Biophys Res Commun* 533: 1419-1426, 2020.
- Wang F, Gu T, Chen Y, Chen Y, Xiong D and Zhu Y: Long non-coding RNA SOX21-AS1 modulates lung cancer progress upon microRNA miR-24-3p/PIM2 axis. *Bioengineered* 12: 6724-6737, 2021.
- Livak KJ and Schmittgen TD: Analysis of relative gene expression data using real-time quantitative PCR and the 2(-Delta Delta C(T)) Method. *Methods* 25: 402-408, 2001.
- Malard B, Lambert C and Kellum JA: In vitro comparison of the adsorption of inflammatory mediators by blood purification devices. *Intensive Care Med Exp* 6: 12, 2018.
- Wu C, Li H, Zhang P, Tian C, Luo J, Zhang W, Bhandari S, Jin S and Hao Y: Lymphatic flow: A potential target in sepsis-associated acute lung injury. *J Inflamm Res* 13: 961-968, 2020.
- Emr BM, Alcamo AM, Carcillo JA, Aneja RK and Mollen KP: Pediatric sepsis update: How are children different? *Surg Infect (Larchmt)* 19: 176-183, 2018.
- Wang J, Yuan X and Ding N: IGF2BP2 knockdown inhibits LPS-induced pyroptosis in BEAS-2B cells by targeting caspase 4, a crucial molecule of the non-canonical pyroptosis pathway. *Exp Ther Med* 21: 593, 2021.
- Guo WF, Lin RX, Huang J, Zhou Z, Yang J, Guo GZ and Wang SQ: Identification of differentially expressed genes contributing to radioresistance in lung cancer cells using microarray analysis. *Radiat Res* 164: 27-35, 2005.
- Liu Z, Han M, Ding K and Fu R: The role of Pim kinase in immunomodulation. *Am J Cancer Res* 10: 4085-4097, 2020.

27. de Vries M, Heijink IH, Gras R, den Boef LE, Reinders-Luinge M, Pouwels SD, Hylkema MN, van der Toorn M, Brouwer U, van Oosterhout AJ and Nawijn MC: Pim1 kinase protects airway epithelial cells from cigarette smoke-induced damage and airway inflammation. *Am J Physiol Lung Cell Mol Physiol* 307: L240-L251, 2014.
28. Wu J, Gan Y, Li M, Chen L, Liang J, Zhuo J, Luo H, Xu N, Wu X, Wu Q, *et al*: Patchouli alcohol attenuates 5-fluorouracil-induced intestinal mucositis via TLR2/MyD88/NF- κ B pathway and regulation of microbiota. *Biomed Pharmacother* 124: 109883, 2020.
29. Lin HY, Tang CH, Chen YH, Wei IH, Chen JH, Lai CH and Lu DY: Peptidoglycan enhances proinflammatory cytokine expression through the TLR2 receptor, MyD88, phosphatidylinositol 3-kinase/AKT and NF- κ B pathways in BV-2 microglia. *Int Immunopharmacol* 10: 883-891, 2010.
30. Hu JT, Lai J, Zhou W, Chen XF, Zhang C, Pan YP, Jiang LY, Zhou YX, Zhou B and Tang ZH: Hypothermia alleviated LPS-induced acute lung injury in Rat models through TLR2/MyD88 pathway. *Exp Lung Res* 44: 397-404, 2018.
31. Ding PH, Wang CY, Darveau RP and Jin L: Porphyromonas gingivalis LPS stimulates the expression of LPS-binding protein in human oral keratinocytes in vitro. *Innate Immun* 19: 66-75, 2013.
32. Narayana Y, Bansal K, Sinha AY, Kapoor N, Puzo G, Gilleron M and Balaji KN: SOCS3 expression induced by PIM2 requires PKC and PI3K signaling. *Mol Immunol* 46: 2947-2954, 2009.
33. Tang X, Cao T, Zhu Y, Zhang L, Chen J, Liu T, Ming X, Fang S, Yuan YF, Jiang L, *et al*: PIM2 promotes hepatocellular carcinoma tumorigenesis and progression through activating NF- κ B signaling pathway. *Cell Death Dis* 11: 510, 2020.
34. Bansal K, Kapoor N, Narayana Y, Puzo G, Gilleron M and Balaji KN: PIM2 Induced COX-2 and MMP-9 expression in macrophages requires PI3K and Notch1 signaling. *PLoS One* 4: e4911, 2009.
35. Xu HB, Qin B, Zhang J, Chen YJ, Shen WW and Cao LN: Growth differentiation factor 11 relieves acute lung injury in mice by inhibiting inflammation and apoptosis. *Eur Rev Med Pharmacol Sci* 24: 6908-6918, 2020.



This work is licensed under a Creative Commons Attribution-NonCommercial-NoDerivatives 4.0 International (CC BY-NC-ND 4.0) License.